AIAA JOURNAL
Vol. 37, No. 11, November 1999

Basic Development of Hybrid Finite Element Method for Midfrequency Structural Vibrations

Nickolas Vlahopoulos* and Xi Zhao†
University of Michigan, Ann Arbor, Michigan 48109-2145

The theoretical development of a hybrid finite element method is presented. It combines conventional finite element analysis (FEA) with energy FEA (EFEA) to achieve a numerical solution to midfrequency vibrations. In the midfrequency range a system comprises some members that contain several wavelengths and some members with just a few wavelengths within their lengths. The former are considered long members, and they are modeled by the EFEA. The latter are considered short, and they are modeled by the FEA. The new formulation is based on deriving appropriate interface conditions at the joints between sections modeled by the EFEA and the FEA methods. The formulation for one flexural degree of freedom in colinear beams is presented in this fundamental development. The excitation is considered to be applied on a long member, and the response of the entire system is computed. Uncertainty effects are imposed only on the long members of the system. Validation cases for several configurations are presented. They compare closed-form analytical solutions to numerical results produced by the hybrid finite element method. Good correlation is observed for all analyses. The resonant behavior of the short members is captured correctly in the response of the system.

Introduction

THE utilization of numerical methods for structural vibrations in aerospace applications is important because it can reduce development time and lead to better-quality products. The performance of alternative designs can be determined through simulations in both aircraft[1–4] and launch vehicle dynamic applications.[5–8] The frequency spectrum where simulation methods can be utilized for vibration analysis can be divided into three regions: low, mid, and high frequency. The low-frequency region is defined as the frequency range where all components are short with respect to a wavelength (short members). Short members respond with low modal density, and resonant effects are dominant. No uncertainties with respect to the natural frequencies or the dimensions of the short members are considered. Conventional finite element analysis (FEA) is a practical numerical approach for simulating low-frequency vibrations.[9–11]

The high-frequency region is defined as the frequency range where all component members of a system are long with respect to a wavelength. Statistical energy analysis (SEA)[12–16] and energy FEA (EFEA)[17–23] can be used for vibro–acoustic simulations at high frequencies. SEA is an established approach for high-frequency analysis. In SEA, the vibro–acoustic system is divided into subsystems of similar modes. The lumped averaged energy within each subsystem composes the primary SEA variable. EFEA is a recent development for high-frequency analysis.[17–23] In EFEA, the primary variable is defined as the time- and space-averaged energy density. The governing differential equations are developed with respect to the energy density, and a finite element approach is employed for the numerical solution. Both methods provide meaningful results for the ensemble-average response[24] when all of the members in the system have high modal density. They represent a modal (SEA) and a wave approach (EFEA) for addressing high-frequency analysis.

The midfrequency region is defined as the frequency range where some of the components of a system are long and other members are short. In the midfrequency range, the FEA method requires a prohibiting large number of elements to perform an analysis due to the presence of the long members. The formulations of the energy methods (SEA and EFEA) contain assumptions that are valid when all components of a system have high modal density. Based on the condition of high modal density, the SEA formulation considers the normal modes within a frequency band as equally spaced, containing the same amount of energy, and demonstrating an equal amount of damping.[16] The condition of a small wavelength with respect to the dimension of a member in the EFEA is equivalent to the condition of high modal density in SEA. The requirement for small wavelength in the EFEA allows to neglect near-field effects in the wave solution during the development of the governing differential equations. Thus, the energy methods cannot capture the resonant effects in the behavior of a system in the midfrequencies. The resonant effects are generated from the presence of the short members.

In the energy methods, the amount of power transferred between members at a joint is defined in terms of coupling loss factors (in SEA) or power transfer coefficients (in EFEA). The process that computes the values of the coupling loss factors or the power transfer coefficients employs analytical solutions of semi-infinite members to define the power transfer characteristics of each joint.[25] The computations are meaningful when the members connected at the joint have high modal density. The requirement for high modal density is necessary because the information produced by the analytical solutions of the semi-infinite members captures the characteristics of power flow between members when the members demonstrate an equal amount of coupling between their normal modes. If large differences exist in the power flow due to the distinct resonant behavior of the short members, then the power transfer characteristics cannot be captured properly from analytical solutions of semi-infinite members. In addition, the behavior of the short members cannot be captured correctly by the energy methods because the resonant effects that are important for the overall behavior of a short member are neglected in the current form of the energy methods.

In the past, conventional finite element models have been employed to determine the SEA coupling loss factors[26–31] or the EFEA power transfer coefficients[22] instead of the analytical solutions of semi-infinite members. Specifically, SEA coupling loss factors have been computed through finite element computations for assemblies of fully connected plates,[26,29] for beam junctions,[27] for interfaces between structural and acoustic subsystems,[30] for the sound transmission between walls in a building,[28] and for connections between rods.[31] EFEA power transfer coefficients have been computed through finite element computations for spot-welded connections.[22] The rationale in all of these developments is to employ conventional FEA because FEA can capture the coupling mechanism when the

Received 17 November 1998; revision received 29 March 1999; accepted for publication 12 April 1999.

*Assistant Professor, Department of Naval Architecture and Marine Engineering, 2600 Draper Road.

†Graduate Student Research Assistant, Department of Naval Architecture and Marine Engineering, 2600 Draper Road.

connection between members presents a complexity that cannot be accounted for by the analytical solutions of semi-infinite members. The approach of utilizing FEA for computing the power transfer characteristics is the only computational option for complex or discontinuous joints, and this approach provides an alternative to evaluating the power transfer characteristics through testing.

An approach based on creating a statistical Green kernel for a boundary element formulation for assembled rods and beams in the midfrequency range has been presented.[32] The statistical Green kernel is constructed based on random mechanical constants. The fundamental solution is then considered as a random function. A direct boundary element approach is employed to achieve numerical solution. Examples of analyzing a single rod, two colinear rods, and a single beam were presented.[32]

The concept of combining an FEA and an SEA formulation for developing a hybrid approach has been presented.[33] The lack of compatibility at the joint between the SEA variables and the FEA variables became a main issue. An optimization routine was developed to approximate the compatibility at the joint between the SEA and the FEA variables.

A fundamentally new formulation is developed here for midfrequency analysis. It is based on coupling conventional FEA models of short members to EFEA models of long members. The ensemble-average response of the long members and the resonant behavior of the short members are captured by the new hybrid formulation. The joints between long and short members are modeled by combining analytical solutions of semi-infinite members that represent the long members to FEA numerical models for the short members. Two sets of data are produced from the developed coupling process. The first set comprises power transfer coefficients for each EFEA member at a joint with a short member. The computed power transfer coefficients contain the effect of the resonant behavior of the short members and the damping that can be present in the short members. The second set of data comprises relationships between the primary variable of the EFEA model at a joint between long and short members and the primary variables of the FEA model at the same joint. Because the EFEA is based on a wave formulation, EFEA lends itself for developing compatibility conditions at a joint with the FEA model of a short member. The wave solution and the FEA solution can be coupled through displacement compatibility conditions at the joint. Another major advantage offered from the wave-based formulation of the EFEA is the distinction between the energy (and the power) associated with the left and the right traveling waves. At a joint between a long and a short member only the energy associated with the impinging wave contributes to the excitation of the short member. Thus, when multiple members are connected together, effects of power reinjection[24] and indirect power flow[34] can be captured correctly by the hybrid finite element solution.

The power transfer coefficients for joints between long members are evaluated by the traditional EFEA approach that is based on analytical solutions of semi-infinite members. The power transfer coefficients that characterize all of the joints are inserted in the EFEA global system of equations. Thus, the solution for the long members accounts for the resonant and dissipative behavior of the short members during the flow of power through the system. Once the primary variables of the EFEA solution have been determined on all of the long members, appropriate boundary conditions are generated for the FEA models of the short members. The excitation is considered to be applied on any long member. When multiple long members are connected with a short member, the excitations that they apply on the short member are treated as incoherent. This is appropriate because by definition the long members contain a large number of wavelengths within their dimension and their ensemble-average response is computed. Numerical solutions of the new hybrid finite element formulation are compared successfully to closed-form analytical solutions for several combinations of midfrequency ranges and beam assemblies. Satisfactory correlation is observed between numerical and analytical results.

Background on EFEA

Because the EFEA formulation for high-frequency analysis constitutes an integral component of the new hybrid development, some background information on the EFEA is presented. Although a variety of members can be represented in EFEA,[17–21] only the formulation associated with one flexural degree of freedom of a beam will be overviewed. It is representative of the EFEA formulation, and it is necessary for explaining the new midfrequency development presented in the following section. The energy density and the power flow are expressed in terms of the far-field displacement solution[19,34]:

$$W(x,t) = (Ae^{-ikx} + Ce^{ikx})e^{i\omega t} \tag{1}$$

where $W(x,t)$ is the far-field displacement solution (function of x and t), A the amplitude of the right traveling far-field wave, C the amplitude of the left traveling far-field wave, k the complex flexural wave number of the beam, and ω the radial frequency. The energy density constitutes the primary variable in formulating the governing differential equation. The energy density averaged over a period can be expressed in terms of the far-field displacement solution as[19]

$$\langle e \rangle = \frac{1}{4}\frac{EI}{S}\left\{\frac{\partial^2 W}{\partial x^2}\left(\frac{\partial^2 W}{\partial x^2}\right)^*\right\} + \frac{1}{4}\rho\left\{\frac{\partial W}{\partial t}\left(\frac{\partial W}{\partial t}\right)^*\right\} \tag{2}$$

where $\langle e \rangle$ is the time-averaged energy density, EI is the flexural rigidity of the beam, S is the cross-sectional area of the beam, ρ is the mass density per unit volume, $\langle\,\rangle$ indicates time averaging over a period, and $()^*$ indicates the conjugate of a complex number. The time-averaged power flow for flexural waves in a beam is also expressed in terms of the far-field displacement solution[19]

$$\langle q \rangle = \frac{1}{2}EI\,\mathrm{Re}\left\{\frac{\partial^3 W}{\partial x^3}\left(\frac{\partial W}{\partial t}\right)^* - \frac{\partial^2 W}{\partial x^2}\left(\frac{\partial^2 W}{\partial x \partial t}\right)^*\right\} \tag{3}$$

where $\langle q \rangle$ is the time-averaged power flow.

The far-field displacement [Eq. (1)] can be substituted into Eqs. (2) and (3). By integrating the new expressions over one wavelength, equations can be derived for the time- and space-averaged energy density and power flow $\langle \bar{e} \rangle$ and $\langle \bar{q} \rangle$ respectively, where the overbar indicates space averaging over a wavelength. From these expressions, a relationship can be derived as[17,19,20]

$$\langle \bar{q} \rangle = \frac{-4c_b^2}{\eta\omega}\frac{\mathrm{d}\langle \bar{e} \rangle}{\mathrm{d}x} \tag{4}$$

where $\langle \bar{q} \rangle$ is the time- and space-averaged power flow, $\langle \bar{e} \rangle$ the time- and space-averaged energy density, η the hysterisis damping factor, and c_b the phase speed of bending waves. $\langle \bar{q} \rangle$ and $\langle \bar{e} \rangle$ will be referred to as power flow and energy density, respectively, in this paper. The time- and space-averaged dissipated power $\langle \bar{\Pi}_{\mathrm{diss}} \rangle$ can be associated to the corresponding energy density[25]:

$$\langle \bar{\Pi}_{\mathrm{diss}} \rangle = \eta\omega\langle \bar{e} \rangle \tag{5}$$

An energy balance at the steady state results in[17,19,20]

$$\langle \bar{Q}_{\mathrm{in}} \rangle = \langle \bar{\Pi}_{\mathrm{diss}} \rangle + \frac{\mathrm{d}\langle \bar{q} \rangle}{\mathrm{d}x} \tag{6}$$

where $\langle \bar{Q}_{\mathrm{in}} \rangle$ is the distributed input power per unit length over the beam (function of x). Substituting Eqs. (4) and (5) into Eq. (6) results in the governing differential equation for the time- and space-averaged energy density:

$$\frac{-c_g^2}{\eta\omega}\frac{\mathrm{d}^2\langle \bar{e} \rangle}{\mathrm{d}x^2} + \eta\omega\langle \bar{e} \rangle = \langle \bar{Q}_{\mathrm{in}} \rangle \tag{7}$$

where c_g is the group speed of the bending waves. A finite element approach is employed for solving Eq. (7) numerically, resulting in[35]

$$\lfloor E^e \rfloor_i \{e^e\}_i = \{F^e\}_i + \{Q^e\}_i \tag{8}$$

where superscript e indicates element-based quantities, subscript i indicates the ith element, $\{e^e\}_i$ is the vector of nodal values for the time- and space-averaged energy density for the ith element, $\lfloor E^e \rfloor_i$ is the system matrix for the ith element, $\{F^e\}_i$ is the vector of input power at the nodal locations of the ith element, and $\{Q^e\}_i$

is the vector of power flow at the boundary locations of the ith element. $\{Q^e\}_i$ provides the mechanism for connecting elements together across discontinuities because at the joint locations the energy density is discontinuous, and the coupling is achieved by accounting for continuity in the power flow.

In the conventional finite element formulations, the continuity of the primary variables of the analysis at the nodes between elements is utilized to assemble the global system matrix. In EFEA, the continuity condition applies to the energy density only if the geometry and the material properties do not change, i.e., in any place other than the location of a joint. When the energy density is continuous, the element equations (8) can be assembled in the conventional FEA manner. At positions where different members are connected, or at locations of discontinuities, the energy density is discontinuous. The corresponding boundary between the elements defines a joint location. Therefore, during the assembly of the global system the element matrices do not couple, and the values of the power flow at the common node do not overlap to cancel each other. Instead, they remain as variables on the right-hand side of the equation:

$$\begin{bmatrix} [E^e]_i & \\ & [E^e]_j \end{bmatrix} \begin{Bmatrix} \{e^e\}_i \\ \{e^e\}_j \end{Bmatrix} = \begin{Bmatrix} \{F^e\}_i \\ \{F^e\}_j \end{Bmatrix} + \begin{Bmatrix} \{Q^e\}_i \\ \{Q^e\}_j \end{Bmatrix} \tag{9}$$

A special procedure is used for assembling the element matrix into the global matrix equations.[35] Two interelement nodes are placed at the joint between two coupled beam elements. Therefore, two energy density values are present at the joint. In the case of multiple coupled structural elements, multiple nodes are placed at the joint. A specialized joint element equation is developed to formulate the connection between the discontinuous primary variables at the joint. The values of the power flow at the interelement nodes corresponding to the two adjacent elements are expressed in terms of the corresponding energy densities:

$$\begin{Bmatrix} Q^e_{ic} \\ Q^e_{jc} \end{Bmatrix} = [J]^i_j \begin{Bmatrix} e^e_{ic} \\ e^e_{jc} \end{Bmatrix} \tag{10}$$

where subscript c indicates the common node between elements i and j, and $[J]^i_j$ is the joint matrix expressing the mechanism of energy transfer between elements i and j. Its coefficients are computed by power transfer coefficients derived from analytical solutions of semi-infinite members fully connected to each other and by taking into account the continuity of the power flow across the joint. Introducing Eq. (10) into Eq. (9) results in

$$\left(\begin{bmatrix} [E^e]_i & \\ & [E^e]_j \end{bmatrix} + [JC]^i_j \right) \begin{Bmatrix} \{e^e\}_i \\ \{e^e\}_j \end{Bmatrix} = \begin{Bmatrix} \{F^e\}_i \\ \{F^e\}_j \end{Bmatrix} \tag{11}$$

where $[JC]^i_j$ is the coupling matrix comprising the coefficients of $[J]^i_j$ positioned in the appropriate locations. Solution to the global finite element system of equations results in evaluating the distribution of the energy density over the entire system. It has been demonstrated[23] that EFEA computations produce results similar to SEA solutions[8] for complex structural systems. Thus, the EFEA constitutes an attractive alternative for high-frequency analysis to the established SEA approach. In addition, due to the wave-based formulation of the EFEA, it is possible to develop appropriate coupling boundary conditions with low-frequency FEA models as presented in this work. Thus, the EFEA offers a significant advantage in formulating midfrequency solutions. This concludes the overview of the current state[17–23,35] of numerical methodologies developed for EFEA.

Development of a Midfrequency Formulation

In the midfrequency range, a system comprises both long and short members. The challenge stems from the following two obstacles:

1) When an energy approach (SEA or EFEA) is utilized to model the behavior of the system, the results will be incorrect in the midfrequency because the assumptions for high modal density inherent in both theories are violated by the existence of the short members. Consequently, the overall accuracy of the system solution will deteriorate.

2) If a discrete solution (FEA) is used for the simulation, then the existence of the long members creates the requirement of having a large number of elements in the model, and the analysis becomes infeasible.

The primary concept of the work here is to utilize low-frequency models (FEA) for deriving energy information for the short members and to integrate them with EFEA models presenting the long members. Because of the presence of the long members in the system, the response of all members will remain incoherent inasmuch as the short members will be subjected to an incoherent excitation at the points where they are connected to the long members. The algorithm presented considers the external excitation applied on any long member. Previous work has demonstrated how low-frequency vibro–acoustic models can be analyzed when they are subjected to incoherent excitation.[5] The EFEA is selected to be coupled with the low-frequency methods because it is based on a spatial discretization of the system that is being modeled. Thus, it is possible to develop appropriate interface conditions at the joints between the primary variables of the EFEA models of the long members and the FEA models of the short members.

In this section, the concept of combining conventional FEA with EFEA is developed theoretically for one flexural degree of freedom in systems of colinear beams. The connection between the long and short members is considered to exhibit the same characteristics as a connection between a semi-infinite member with structural properties identical to the long member and the actual short member. Representing a long member as semi-infinite during the derivation of the power transfer characteristics of a joint is consistent with the EFEA formulation of joints between long members and with the derivation of SEA coupling loss factors from wave solutions of semi-infinite members. In the joint formulation of the hybrid method, the short member (which is modeled by finite elements) does include damping; thus, both the resonant and the dissipative characteristics of the short members are captured in the derivation of the power transfer coefficients. Two objectives are accomplished from the hybrid joint formulation.

First, the effect of the short members on the behavior of the long members is accounted for by deriving a relationship between the amount of power flow and energy density at all joint locations between long and short members. The resonant and damping characteristics of the short members, the boundary conditions imposed on the short members, and the frequency of the analysis impact the computations. The relationship between the power flow and the energy density at a joint is employed for deriving the EFEA power transfer coefficients for the long members at the joints with the short members. The power transfer coefficients of the long members derived by the hybrid joint formulation account for all of the characteristics of the short members.

Second, the energy density of the wave impinging from a long member at a joint with a short is associated to the displacement and slope of the short member. Thus, the energy distribution over the long members dictates appropriate boundary conditions imposed on the low-frequency analysis of the short members. The response of a short member subjected to excitation imposed at its joints with multiple long members is computed by considering the reverberant nature of the vibrational field present in all of the long members.

The overall hybrid finite element formulation can be divided into three sections.

The first section is the hybrid formulation of a joint between long and short members. The relationship between the power flow and the energy density at the joint between a long and a short member is formulated. The EFEA power transfer coefficients for the long member are derived. The capability of the short member to dissipate energy is taken into account during the derivation of the power transfer coefficients. During the same computational process, a relationship is also developed between the primary variables of the FEA formulation of the short member and the primary variable of the EFEA formulation of the long member at the common joint. The relationship between the primary variables of the two formulations provides the mechanism of prescribing excitation on the short members. Because only one wave type in colinear beams is considered in this basic development, up to two long members can be connected to a short one.

The second section is the numerical solution for the long members. The global EFEA system matrix is assembled for all of the long members. Power transfer coefficients derived from analytical solutions of semi-infinite members are utilized for generating the coupling matrix $[JC]^i_j$ between long members. Power transfer coefficients derived from the hybrid joint formulation are employed for evaluating the coupling matrix $[JC]^i_j$ for the long members that are connected to short ones. The external excitation is considered to be applied on long members, and the EFEA solution for all of the long members is computed. The influence of the short members on the behavior of the long is captured through the EFEA power transfer coefficients computed from the hybrid formulation of the joints between long and short members.

The third section is the numerical solution for the short members. The EFEA solution of the long members provides the EFEA primary variables at the joints between long and short members. The EFEA energy density at the joints is employed for determining the boundary conditions imposed on the FEA primary variables of the short members. Because of the wave-based approach of the EFEA formulation, the amount of energy associated only with the wave impinging in the joint can be identified from the energy density that constitutes the primary variable of the EFEA formulation. Only the energy associated with the impinging wave is employed for defining the excitation exerted on the short member. Thus, it is possible to account for power reinjection effects when multiple long members are present in the system. When multiple long members are connected to a short member, the boundary conditions that they impose on the short member are treated as incoherent because they originate from the reverberant fields that exist within each one of the long members. The boundary conditions imposed on the short members ensure continuity of power flow between all of the members.

Hybrid Formulation for a Joint Between Long and Short Members

A finite element discretization is utilized for modeling the short member. The equation of motion can be written in matrix form as

$$[-\omega^2[M] + i\omega[C] + [K]]\{u\} = \{R\} + \{F_R\}$$

$$\Rightarrow [ST]\{u\} = \{R\} + \{F_R\} \tag{12}$$

where $[M]$, $[C]$, and $[K]$ are the mass, damping, and stiffness matrices, respectively; $\{u\}$ is the displacement of vibration; $[ST]$ is the global structural system matrix including the mass, damping, and stiffness effects; $\{R\}$ is the vector of reaction forces and moments imposed by supports; and $\{F_R\}$ is the vector of external forces applied at the boundaries of the member by the adjacent long members. Equation (12) can be partitioned into the degrees of freedom at the interface with the long members and the remaining degrees of freedom. Because the current development accounts for one bending degree of freedom in colinear beams, the maximum number of long members connected to a short is two. Therefore, the equations of the hybrid joint formulation are presented for the case of two long members connected to a short member. Because the FEA method is employed to model the short members, several of them can be connected to each other and placed between long ones. There is no inherent limitation in extending the concept developed to a large number of long members and degrees of freedom. Partitioning Eq. (12) for a short member results in

$$\begin{bmatrix} [ST_{11}] & [ST_{12}] \\ [ST_{21}] & [ST_{22}] \end{bmatrix} \begin{Bmatrix} u_m \\ \dfrac{du_m}{dx} \\ u_n \\ \dfrac{du_n}{dx} \\ \{u_2\} \end{Bmatrix} = \begin{Bmatrix} 0 \\ 0 \\ 0 \\ 0 \\ \{R_2\} \end{Bmatrix} + \begin{Bmatrix} F_m \\ M_m \\ F_n \\ M_n \\ \{0\} \end{Bmatrix} \tag{13}$$

where the subscript m corresponds to the displacement u_m and its derivative du_m/dx at the left joint with a long member; the subscript n corresponds to the displacement u_n and its derivative du_n/dx at the right joint with a long member; F_m, M_m, F_n, and M_n are forces and moments exerted from the long members on the short member at the two joint locations; subscript 1 corresponds to the FEA degrees of freedom at the joints; subscript 2 corresponds to the remaining FEA degrees of freedom, and $\{R_2\}$ are the forces and moments applied by external excitation or supports on the FEA degrees of freedom at any location other than the joints. At the current state of the development, no excitation forces are considered to be applied on the short members; thus, $\{R_2\} = \{0\}$. From the lower part of Eq. (13), $\{u_2\}$ can be expressed in terms of the FEA degrees of freedom at the joints and then substituted in the upper part. This results in

$$[S] \begin{Bmatrix} u_m \\ \dfrac{du_m}{dx} \\ u_n \\ \dfrac{du_n}{dx} \end{Bmatrix} = \begin{Bmatrix} F_m \\ M_m \\ F_n \\ M_n \end{Bmatrix} \tag{14}$$

where $[S] = [[ST_{11}] - [ST_{12}][ST_{22}]^{-1}[ST_{21}]]$ is the condensed FEA system of equations.

The interaction forces and moments F_m, M_m, F_n, and M_n between the long and the short members at the two joints can be expressed in terms of the primary variables of the FEA formulation at the joints and the entries of matrix $[S]$:

$$\begin{aligned} S_{11}u_m + S_{12}\frac{du_m}{dx} + S_{13}u_n + S_{14}\frac{du_n}{dx} &= F_m \\ S_{21}u_m + S_{22}\frac{du_m}{dx} + S_{23}u_n + S_{24}\frac{du_n}{dx} &= M_m \\ S_{31}u_m + S_{32}\frac{du_m}{dx} + S_{33}u_n + S_{34}\frac{du_n}{dx} &= F_n \\ S_{41}u_m + S_{42}\frac{du_m}{dx} + S_{43}u_n + S_{44}\frac{du_n}{dx} &= M_n \end{aligned} \tag{15}$$

where S_{ij} is the entry in the ith row and jth column of matrix $[S]$.

The system of Eq. (15) constitutes the foundation for deriving: 1) EFEA power transfer coefficients for the long members that include the resonant effects of the short members and 2) relationships between EFEA and FEA primary variables at the joints.

Derivation of EFEA Power Transfer Coefficients at Joints Between Long and Short Members

The formulation of the power transfer coefficients between two long members connected by a short one is presented. Two semi-infinite members with no damping are coupled to the FEA model of the short member. The FEA model includes any damping characteristics present in the short member. The system of equations representing the semi-infinite members and the short member is employed to calculate the amount of reflected and transmitted power associated with an impinging wave from each semi-infinite member. By considering a wave incident to the joint from the left semi-infinite member, the analytical expressions for the two semi-infinite members become

$$W^m_m(x,t) = w^m_m(x)e^{i\omega t} = \left(A^m_m e^{-ik_m x} + C^m_m e^{ik_m x} + D^m_m e^{k_m x}\right)e^{i\omega t} \tag{16}$$

$$W^m_n(x,t) = w^m_n(x)e^{i\omega t} = \left(C^m_n e^{-ik_n(x-l_s)} + D^m_n e^{-k_n(x-l_s)}\right)e^{i\omega t} \tag{17}$$

where the superscript m is associated with the incident wave; subscripts m and n indicate the left and right semi-infinite members, respectively; l_s is the length of the short member; and constants A, C, and D are the amplitudes of waves developed within the semi-infinite members. The wave numbers can be obtained by the equations

$$k_m = \left[\frac{\omega^2 \rho_m S_m}{E_m I_m}\right]^{\frac{1}{4}} \tag{18}$$

$$k_n = \left[\frac{\omega^2 \rho_n S_n}{E_n I_n}\right]^{\frac{1}{4}} \tag{19}$$

where ρ is the density, S the cross sectional area, and EI the bending rigidity.

Continuity of displacement and slope and equilibrium of force and moment at the two ends of the short member are expressed in terms of the displacements and the slopes at the two ends of the short beam, u_m^m, $\mathrm{d}u_m^m/\mathrm{d}x$, u_n^m, and $\mathrm{d}u_n^m/\mathrm{d}x$, and the unknown coefficients and C_m^m, D_m^m, C_n^m, and D_n^m. A_m^m is the amplitude of the impinging wave, and it is utilized as reference in the computations. The continuity conditions for the displacement and the slope and the equilibrium of force and moment at the joints between the short and the semi-infinite members result in a system of eight equations between the primary variables of the FEA formulation, u_m^m, $\mathrm{d}u_m^m/\mathrm{d}x$, u_n^m, and $\mathrm{d}u_n^m/\mathrm{d}x$; the unknown coefficients associated with the reflected wave in the left semi-infinite member (C_m^m, D_m^m); and the unknown coefficients associated with the transmitted wave in the right semi-infinite member (C_n^m, D_n^m). The system of equations can be expressed in matrix form as

$$\begin{bmatrix} 1 & 0 & 0 & 0 & -1 & -1 & 0 & 0 \\ 0 & -1 & 0 & 0 & ik_m & k_m & 0 & 0 \\ 0 & 0 & 1 & 0 & 0 & 0 & -1 & -1 \\ 0 & 0 & 0 & 1 & 0 & 0 & ik_n & k_n \\ S_{11}^m & S_{12}^m & S_{13}^m & S_{14}^m & i(EI)_m k_m^3 & -(EI)_m k_m^3 & 0 & 0 \\ S_{21}^m & S_{22}^m & S_{23}^m & S_{24}^m & -(EI)_m k_m^2 & (EI)_m k_m^2 & 0 & 0 \\ S_{31}^m & S_{32}^m & S_{33}^m & S_{34}^m & 0 & 0 & i(EI)_n k_n^3 & -(EI)_n k_n^3 \\ S_{41}^m & S_{42}^m & S_{43}^m & S_{44}^m & 0 & 0 & (EI)_n k_n^2 & -(EI)_n k_n^2 \end{bmatrix} \begin{Bmatrix} u_m^m \\ \mathrm{d}u_m^m/\mathrm{d}x \\ u_n^m \\ \mathrm{d}u_n^m/\mathrm{d}x \\ C_m^m \\ D_m^m \\ C_n^m \\ D_n^m \end{Bmatrix} = \begin{Bmatrix} 1 \\ ik_m \\ 0 \\ 0 \\ i(EI)_m k_m^3 \\ (EI)_m k_m^2 \\ 0 \\ 0 \end{Bmatrix} A_m^m \tag{20}$$

By solving the system of Eq. (20), each one of the eight unknowns can be expressed in terms of the coefficient A_m^m, which is associated with the impinging wave:

$$u_m^m = a_1^m A_m^m, \qquad \frac{\mathrm{d}u_m^m}{\mathrm{d}x} = a_2^m A_m^m, \qquad u_n^m = a_3^m A_m^m$$

$$\frac{\mathrm{d}u_n^m}{\mathrm{d}x} = a_4^m A_m^m, \qquad C_m^m = a_5^m A_m^m, \qquad D_m^m = a_6^m A_m^m$$

$$C_n^m = a_7^m A_m^m, \qquad D_n^m = a_8^m A_m^m \tag{21}$$

The power transmission coefficient τ_{mn} is the ratio of the transmitted power over the incident power. The power reflection coefficient r_{mm} is the ratio of the reflected power over the incident power. Hence, the power transfer coefficient τ_{mn} for the right member n due to the incident wave in the left member m is

$$\tau_{mn} = \frac{q_{\mathrm{tran}}^m}{q_{\mathrm{inc}}^m} = \frac{(EI)_n k_n^3 \omega |C_n^m|^2}{(EI)_m k_m^3 \omega |A_m^m|^2} = \frac{(EI)_n k_n^3}{(EI)_m k_m^3} \left| \frac{C_n^m}{A_m^m} \right|^2$$

$$= \frac{(EI)_n k_n^3}{(EI)_m k_m^3} |a_7^m|^2 \tag{22}$$

The reflection coefficient r_{mm} in the left member m due to the incident wave in the same member is

$$r_{mm} = \frac{q_{\mathrm{refl}}^m}{q_{\mathrm{inc}}^m} = \frac{(EI)_m k_m^3 \omega |C_m^m|^2}{(EI)_m k_m^3 \omega |A_m^m|^2} = \left| \frac{C_m^m}{A_m^m} \right|^2 = |a_5^m|^2 \tag{23}$$

The derivation of the EFEA power transfer coefficients accounts for the resonant and damping characteristics of the short member. The constants a_5^m and a_7^m that are directly associated to r_{mm} and τ_{mn}, respectively, are computed from the solution to Eq. (20), which includes all of the characteristics of the FEA matrix of the short member condensed to the interface degrees of freedom at the joint.

By considering an incident wave originating from the right semi-infinite member, equations similar to Eqs. (22) and (23) are derived for the power transfer coefficients τ_{nm} and r_{nn}:

$$\tau_{nm} = \frac{q_{\mathrm{tran}}^n}{q_{\mathrm{inc}}^n} = \frac{(EI)_m k_m^3 \omega |C_m^n|^2}{(EI)_n k_n^3 \omega |A_n^n|^2} = \frac{(EI)_m k_m^3}{(EI)_n k_n^3} \left| \frac{C_m^n}{A_n^n} \right|^2$$

$$= \frac{(EI)_m k_m^3}{(EI)_n k_n^3} |a_5^n|^2 \tag{24}$$

$$r_{nn} = \frac{q_{\mathrm{refl}}^n}{q_{\mathrm{inc}}^n} = \frac{(EI)_n k_n^3 \omega |C_n^n|^2}{(EI)_n k_n^3 \omega |A_n^n|^2} = \left| \frac{C_n^n}{A_n^n} \right|^2 = |a_7^n|^2 \tag{25}$$

where superscript n indicates wave impinging from the right semi-infinite member.

Derivation of Relationship Between EFEA and FEA Primary Variables at a Joint Between Long and Short Members

When two long members are connected by a short member, the energy density at the edge of the left member at the joint depends on the right traveling wave and its reflection, but at the same time it depends on the amount of power transmitted from the other long member. Thus, the energy density e_m at the connection of the left semi-infinite member to the short member can be written as

$$e_m = e_m^+ + e_m^- = e_m^+ + \frac{q_m^-}{c_{gm} S_m} = e_m^+ + \frac{1}{c_{gm} S_m} \left(r_{mm} q_m^+ + \tau_{nm} q_n^- \right)$$

$$= (1 + r_{mm}) e_m^+ + \frac{c_{gn} S_n}{c_{gm} S_m} \tau_{nm} e_n^- \tag{26}$$

where c_{gm} is the group speed of the left member and c_{gn} is the group speed of the right member. In a similar manner,

$$e_n = \frac{c_{gm} S_m}{c_{gn} S_n} \tau_{mn} e_m^+ + (1 + r_{nn}) e_n^- \tag{27}$$

Combining Eqs. (26) and (27) in matrix form results in

$$\begin{Bmatrix} e_m \\ e_n \end{Bmatrix} = \begin{bmatrix} (1 + r_{mm}) & \dfrac{c_{gn} S_n}{c_{gm} S_m} \tau_{nm} \\ \dfrac{c_{gm} S_m}{c_{gn} S_n} \tau_{mn} & (1 + r_{nn}) \end{bmatrix} \begin{Bmatrix} e_m^+ \\ e_n^- \end{Bmatrix} = [E] \begin{Bmatrix} e_m^+ \\ e_n^- \end{Bmatrix} \tag{28}$$

The values for e_m and e_n are computed by the EFEA analysis for the long members. In the EFEA analysis, the power transfer coefficients at joints with short members capture the resonant behavior and the dissipation occurring in the short members. The values for e_m^+ and e_n^- are computed by Eq. (28), and they are utilized to prescribe the excitation on the short member. Only the component of the energy density associated with the wave impinging on the short member is employed for defining the excitation on the short member. The excitation applied from each long member on the short member is considered as incoherent because it originates from the reverberant field of each long member. The energy densities e_m^+ of the impinging wave from the left semi-infinite member can be associated with the amplitude of the wave as

$$e_m^+ = \tfrac{1}{2} \rho_m \omega^2 |A_m^m|^2 \tag{29}$$

Equations (21) and (29) can be employed to develop relationships between the FEA primary variables at the two ends of the short member and the amount of energy density associated with the impinging wave at the joint:

$$u_m^m = a_1^m A_m^m, \qquad \frac{\mathrm{d}u_m^m}{\mathrm{d}x} = a_2^m A_m^m$$

$$u_n^m = a_3^m A_m^m, \qquad \frac{\mathrm{d}u_n^m}{\mathrm{d}x} = a_4^m A_m^m \tag{30}$$

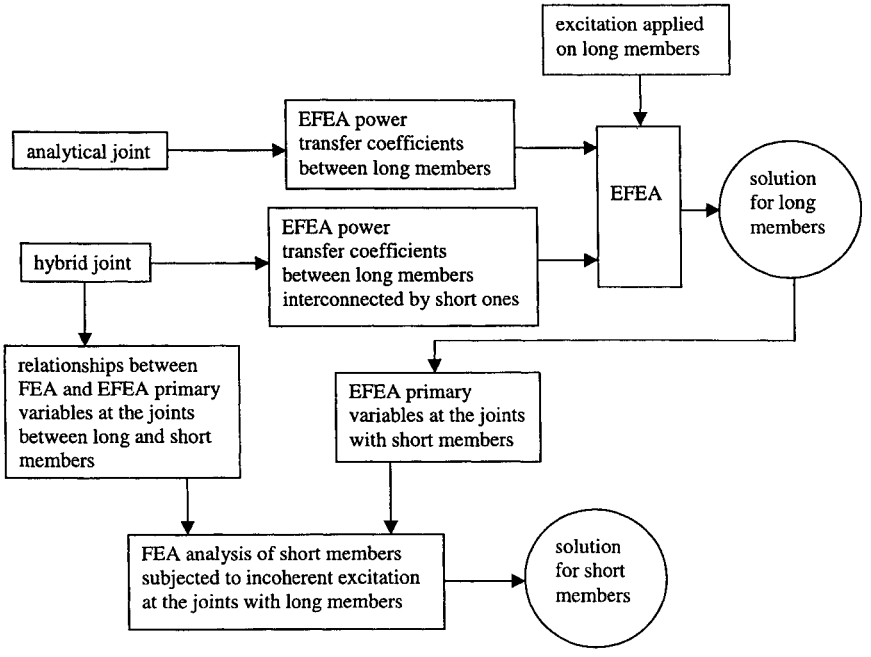

Fig. 1 Flowchart of the hybrid computational process.

The relative phase information within the short member is retained in the computations because the constants a_i^m have complex values. In a similar manner, by considering the impinging wave from the right semi-infinite member, a set of relationships can be developed between the EFEA energy density associated with the impinging wave at the edge of the right long member at the joint and the FEA primary variables at the two ends of the short member:

$$e_n^- = \tfrac{1}{2}\rho_n\omega^2\left|A_n^n\right|^2, \qquad u_m^n = a_1^n A_n^n, \qquad \frac{\mathrm{d}u_m^n}{\mathrm{d}x} = a_2^n A_n^n$$

$$u_n^n = a_3^n A_n^n, \qquad \frac{\mathrm{d}u_n^n}{\mathrm{d}x} = a_4^n A_n^n \tag{31}$$

System Solution

The excitation is considered to be applied on long members. The global EFEA system matrix is assembled for all of the long members. Power transfer coefficients evaluated from analytical solutions of semi-infinite members are utilized for generating the coupling matrices $[JC]_j^i$ between long members. The power transfer coefficients derived by Eqs. (22–25) for the joints between short and long members are employed for developing the joint matrices $[JC]_j^i$ for long members connected through short ones. The power transfer coefficients from Eqs. (22–25) include the effect of the resonant and dissipative characteristics of the short members in the power transfer mechanism. The EFEA system of equations is solved first. The distribution of the energy density over all of the long members is evaluated. Equations (29–31) are employed to identify appropriate boundary conditions on each short member of the system due to the distribution of the energy density on the long ones. Each short member is subjected to incoherent excitation from the presence of a certain amount of energy density at every interface with a long member. The boundary conditions originating from the energy density on the left edge of a short member are imposed first [Eqs. (29) and (30)] on each short member. The FEA method is employed to solve for the remaining FEA degrees of freedom $\{u_2^m\}$ as

$$\left\{u_2^m\right\} = -[ST_{22}]^{-1}[ST_{21}]\begin{Bmatrix} u_m^m \\ \dfrac{\mathrm{d}u_m^m}{\mathrm{d}x} \\ u_n^m \\ \dfrac{\mathrm{d}u_n^m}{\mathrm{d}x} \end{Bmatrix} \tag{32}$$

where $\{u_2^m\}$ are the FEA degrees of freedom for a short member subjected to boundary conditions originating from the e_m energy density at the joint with the left long member. In a similar manner, $\{u_2^n\}$ can be computed from boundary conditions originating from the e_n energy density at the joint with the right long member [Eq. (31)]. Because the excitations e_m and e_n are incoherent, the total response and the energy density distribution over the short member are evaluated by adding up the response $\{u_2^m\}$ and $\{u_2^n\}$ on an energy basis. The effects from power reinjected in the long members is accounted for in the solution because Eq. (28) includes, on the left side, terms associated with both reflected power and power transmitted from the other long member. The computation of the total response is equivalent to a random analysis of a linear system subjected to incoherent excitation, i.e., no cross-correlation terms between excitations applied at different positions.[5] Figure 1 summarizes the hybrid computational process.

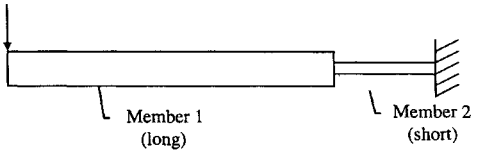

Fig. 2 Two-beam assembly utilized in the validation.

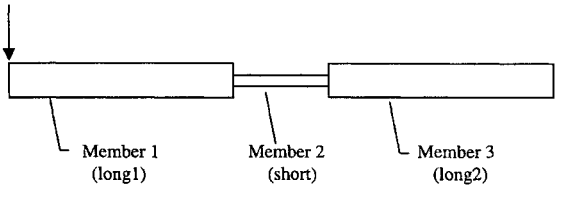

Fig. 3 Three-beam assembly utilized in the validation.

Validation

The validity of the basic research performed is demonstrated by computing the flexural energy of several systems comprising long and short members and comparing the numerical results to analytical solutions. The properties of the beams are selected so that some constitute long members with several wavelengths present within their length, and others can be considered short with only a few wavelengths within their length. Variations of two primary configurations of a two-beam (Fig. 2) and a three-beam (Fig. 3) system are analyzed. The two-beam system comprises a long and a short beam. One end of the short beam is clamped, and the other is

Table 1 Configurations of the systems employed in the validations

System	Length, m		
	Member 1	Member 2	Member 3
1	3	1	NA
2	3	3	NA
3	3	0.5	NA
4	3	0.5	3
5	3	1	3
6	3	1	5.4

Table 2 Cross-sectional properties of beams employed in the validation

Parameter	Long beam	Short beam
Young's modulus of elasticity E, N/m^2	19.5×10^{10}	19.5×10^{10}
Moment of inertia I, m^4	9.365×10^{-10}	5.853×10^{-11}
Mass density ρ, kg/m^3	7700	7700
Damping factor η	0.02	0.02
Cross-sectional area A, m^2	1.935×10^{-4}	0.4839×10^{-4}
Cross-sectional dimensions: width × height, m	0.0254×0.00762	0.0127×0.00381

connected to the long member. Excitation is applied at the free end of the long member. The three-beam system comprises two long beams interconnected by a short one. Free-end boundary conditions are considered for the two ends of the long beams that are not attached to the short member. Excitation is applied at the free end of the left long beam. Several configurations of these two systems with variations imposed on the length of certain members are employed in the validation (Table 1). The hybrid results are compared to analytical solutions. The primary reason for selecting assemblies of colinear beams for initiating the development of the hybrid method is the availability of convenient analytical solutions for validating the theoretical and numerical developments.

To simulate the ensemble-average behavior of the long members in the analytical solution, a 4% variation is introduced in the length of the long members.[36] The ensemble of systems incorporates all of the effects of uncertainty associated with the long members, but it is defined for a specific frequency.[24] In the validation presented here, it is preferred to introduce the uncertainty associated with the long members through an ensemble of systems rather than frequency averaging to better demonstrate in the solution the highly resonant effects of the short member. The cross-sectional properties of the long and the short members are summarized in Table 2. The appropriate properties for the long and the short members employed in the midfrequency analyses are determined by considering several configurations of cross-sectional properties for the two-beam system. For every combination of cross-sectional properties, two systems are evaluated analytically, a long–long and a long–short. The properties of the members are selected in a manner that amplifies the difference between the analytical results obtained for the long–long and the long–short configurations. The rationale for establishing this selection process is for the long–short system to present the largest possible differentiation from the long–long and, thus, the most challenging configuration for testing the new hybrid formulation. In the selected configuration, the short member has lower bending rigidity than the long member. Physically, the selection is justified because the long member can excite the short member considerably more when the latter has lower bending rigidity. The selected configuration also demonstrates that the characterization of a member as long or short depends on both the bending rigidity and its length. In the configuration selected for the validation, the wavelength in the short member is smaller than the wavelength in the long member; however, the lengths of the beams become the determining factor of quantifying them as long or short.

Analytical Solution

The newly developed midfrequency approach (hybrid FEA–EFEA) is utilized to obtain a numerical solution that is compared successfully with an analytical solution. The analytical solution for a system of colinear beams is accomplished by a MATLAB® code. The displacement solutions for each beam are considered. First for a long member,

$$W_l(x,t) = \left(A_l e^{-ik_l x} + B_l e^{-k_l x} + C_l e^{ik_l x} + D_l e^{k_l(x-L_l)}\right)e^{i\omega t} \quad (33)$$

and then for a short member,

$$W_s(x,t) = \left(A_s e^{-ik_s x} + B_s e^{-k_s x} + C_s e^{ik_s x} + D_s e^{k_s(x-L_s)}\right)e^{i\omega t} \quad (34)$$

where $W_l(x,t)$ is the analytical displacement solution of a long member (function of x and t), A_l is the amplitude of the right traveling far-field wave, B_l is the amplitude of the right traveling near-field wave, C_l is the amplitude of the left traveling far-field wave, D_l is the amplitude of the left traveling near-field wave, k_l is the complex flexural wave number of the long member, L_l is the length of the long beam, ω is the radial frequency, and $W_s(x,t)$, A_s, B_s, C_s, D_s, k_s, and L_s are the corresponding expressions for a short member. A separate reference system is utilized for each member. The origin is positioned at the left end of each member. Then the power flow and energy density are expressed in terms of the analytical displacement solution.

Power flow in a beam is transmitted by shear and moment mechanisms. For a long member the time-averaged power associated with the shear force and the moment is

$$\langle q_l \rangle = \frac{1}{2} E_l I_l \,\mathrm{Re}\left\{ \frac{\partial^3 W_l}{\partial x^3}\left(\frac{\partial W_l}{\partial t}\right)^* - \frac{\partial^2 W_l}{\partial x^2}\left(\frac{\partial^2 W_l}{\partial x \partial t}\right)^* \right\} \quad (35)$$

and for a short member is

$$\langle q_s \rangle = \frac{1}{2} E_s I_s \,\mathrm{Re}\left\{ \frac{\partial^3 W_s}{\partial x^3}\left(\frac{\partial W_s}{\partial t}\right)^* - \frac{\partial^2 W_s}{\partial x^2}\left(\frac{\partial^2 W_s}{\partial x \partial t}\right)^* \right\} \quad (36)$$

where subscripts l and s are associated with the long and the short members, respectively.

The total energy density in a transversely vibrating beam is the sum of its potential energy density V and kinetic energy density T. The time-averaged total energy density solution for the long member is

$$\langle e_l \rangle = \frac{1}{4}\frac{E_l I_l}{S_l}\left\{ \frac{\partial^2 W_l}{\partial x^2}\left(\frac{\partial^2 W_l}{\partial x^2}\right)^* \right\} + \frac{1}{4}\rho_l \left\{ \frac{\partial W_l}{\partial t}\left(\frac{\partial W_l}{\partial t}\right)^* \right\} \quad (37)$$

and for a short member is

$$\langle e_s \rangle = \frac{1}{4}\frac{E_s I_s}{S_s}\left\{ \frac{\partial^2 W_s}{\partial x^2}\left(\frac{\partial^2 W_s}{\partial x^2}\right)^* \right\} + \frac{1}{4}\rho_s \left\{ \frac{\partial W_s}{\partial t}\left(\frac{\partial W_s}{\partial t}\right)^* \right\} \quad (38)$$

Then substituting the displacement solutions [Eqs. (33) and (34)] into Eqs. (35) and (36) and calculating time-averaged energy density result in the relationships

$$\begin{aligned}\langle e_l \rangle = {} & \tfrac{1}{4}\left(E_l I_l / S_l\right)\left|k_l^2\right|^2 \left(-A_l e^{-ik_l x} + B_l e^{-k_l x} - C_l e^{ik_l x}\right. \\ & \left. + D_l e^{k_l(x-L_l)}\right)\left(-A_l e^{-ik_l x} + B_l e^{-k_l x} - C_l e^{ik_l x} + D_l e^{k_l(x-L_l)}\right)^* \\ & + \tfrac{1}{4}\rho_l \omega^2 \left(A_l e^{-ik_l x} + B_l e^{-k_l x} + C_l e^{ik_l x} + D_l e^{k_l(x-L_l)}\right) \\ & \times \left(A_l e^{-ik_l x} + B_l e^{-k_l x} + C_l e^{ik_l x} + D_l e^{k_l(x-L_l)}\right)^* \end{aligned} \quad (39)$$

$$\begin{aligned}\langle e_s \rangle = {} & \tfrac{1}{4}\left(E_s I_s / S_s\right)\left|k_s^2\right|^2 \left(-A_s e^{-ik_s x} + B_s e^{-k_s x} - C_s e^{ik_s x}\right. \\ & \left. + D_s e^{k_s(x-L_s)}\right)\left(-A_s e^{-ik_s x} + B_s e^{-k_s x} - C_s e^{ik_s x} + D_s e^{k_s(x-L_s)}\right)^* \\ & + \tfrac{1}{4}\rho_s \omega^2 \left(A_s e^{-ik_s x} + B_s e^{-k_s x} + C_s e^{ik_s x} + D_s e^{k_s(x-L_s)}\right) \\ & \times \left(A_s e^{-ik_s x} + B_s e^{-k_s x} + C_s e^{ik_s x} + D_s e^{k_s(x-L_s)}\right)^* \end{aligned} \quad (40)$$

Finally, the energy density $\langle e_l \rangle$ and $\langle e_s \rangle$ are space averaged over one wavelength to obtain the time- and space-averaged energy density $\langle \bar{e}_l \rangle$ and $\langle \bar{e}_s \rangle$ in the long and the short members, respectively. In all of the analyses, a unit load is applied on the system, and the analytical solution for the ensemble average response is computed. To introduce the ensemble-average behavior of the long members in the analytical solution, a 4% variation[36] is introduced in the length of the long members. The power input into the system is also computed from the analytical solution, and it is defined as excitation in the hybrid and the EFEA computations. Thus, in all three solutions, the system is subjected to the same excitation.

Two-Beam System

An analysis is first performed at 493 Hz, which is a natural frequency for the short member under clamped–free boundary conditions. A detailed comparison between analytical and hybrid results can be performed at a particular frequency where the behavior of the system is expected to be dominated by the highly resonant effects of the short member. Figure 4 presents results from the analytical, the hybrid, and the EFEA computations.

To demonstrate the improvement achieved in the numerical solution by the development of the hybrid formulation, the EFEA is utilized as a representative high-frequency approach to model all of the members of the systems utilized in the validation. The EFEA results demonstrate the deficiency inherent to a high-frequency method when simulating the behavior of a midfrequency system due to its inability to capture the resonant behavior of the short members. It can be observed that the EFEA cannot account for the resonant behavior of the short member in the vicinity of its natural frequency and severely underpredicts its response. The hybrid solution is a significant improvement, and the results correlate well with the analytical solution for both the long and the short members. To demonstrate that the lack of a large number of wavelengths in the short member is the reason for the inaccuracy of the EFEA, the length of the short member is extended (system 2) to increase the number of wavelengths. Both members in the system become long. EFEA results for the average energy density in each one of the two members are presented in Fig. 5 along with analytical results for the frequency range 480–500 Hz. Significant improvement in the correlation can be observed. The average energy density of a member is computed by dividing the total energy of the member by its volume. The average energy density of a member is utilized as a variable that represents its overall behavior at a particular frequency.

Results for the average energy density of the short and the long members of system 1 in the frequency range 477–509 Hz are presented in Fig. 6. By comparison to Fig. 5, it can be observed that the performance of the EFEA deteriorates because the right beam becomes a short member. The EFEA solution severely underpredicts the response of the short member because it can not account for its highly resonant behavior. The hybrid solution agrees very well with the analytical solution. The good correlation demonstrates that the hybrid formulation accurately captures the power transfer mechanism between a long and a short member and the resonant behavior of the short member. In the FEA model of the short member, 40 finite elements are utilized. The results for the total energy in the system are presented in Fig. 7 for the analytical, the hybrid,

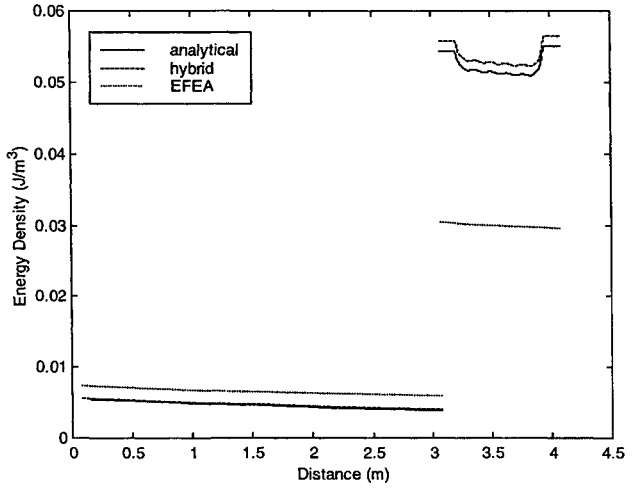

Fig. 4 Analytical, hybrid, and EFEA results for the space-averaged energy density for system 1: 493 Hz.

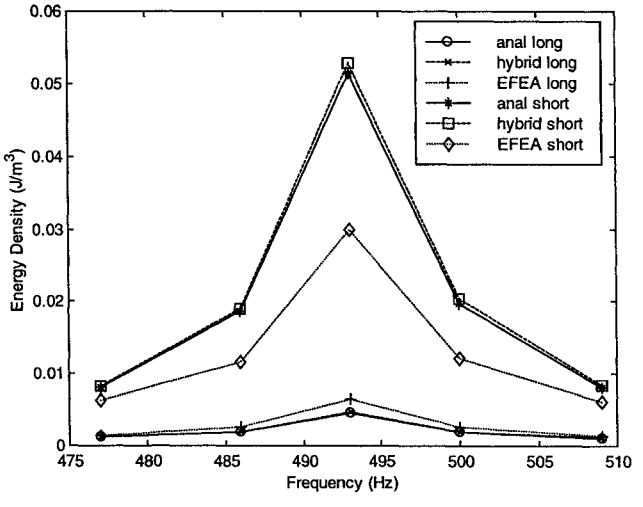

Fig. 6 Analytical, hybrid, and EFEA results for the space-averaged energy density for the members in system 1: 477–509 Hz.

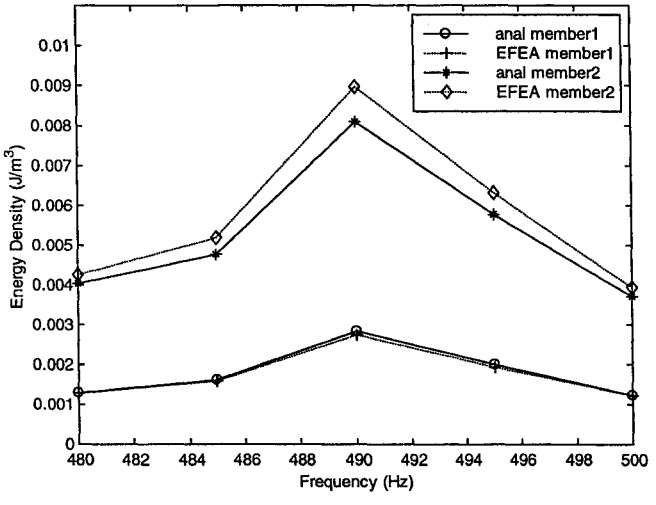

Fig. 5 Analytical and EFEA results for the space-averaged energy density in each member of system 2: 480–500 Hz.

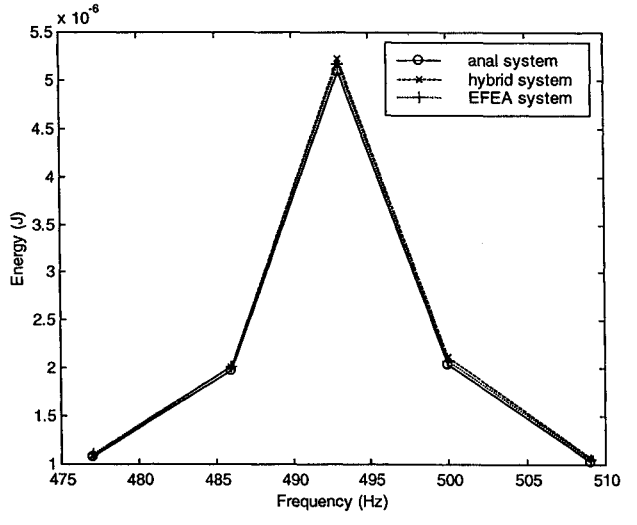

Fig. 7 Analytical, hybrid, and EFEA results for the total energy for system 1: 477–509 Hz.

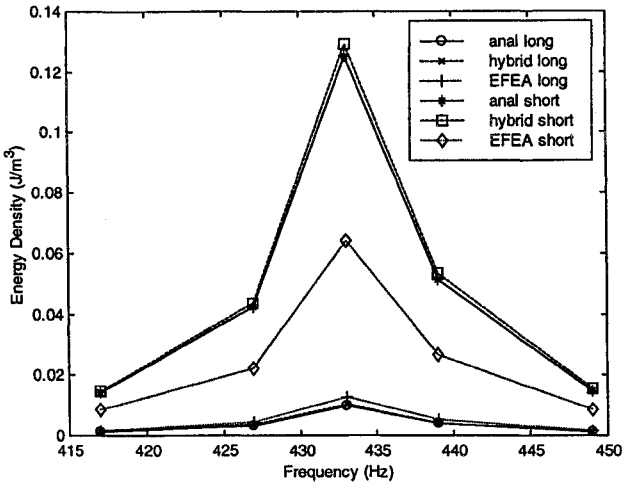

Fig. 8 Analytical, hybrid, and EFEA results for the space-averaged energy density of the beams in system 3: 417–449 Hz.

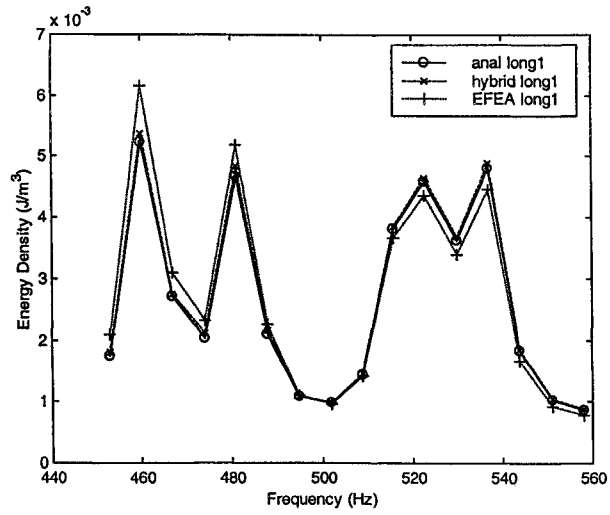

Fig. 10 Analytical, hybrid, and EFEA results for the space-averaged energy density for the left long beam in system 4: 453–558 Hz.

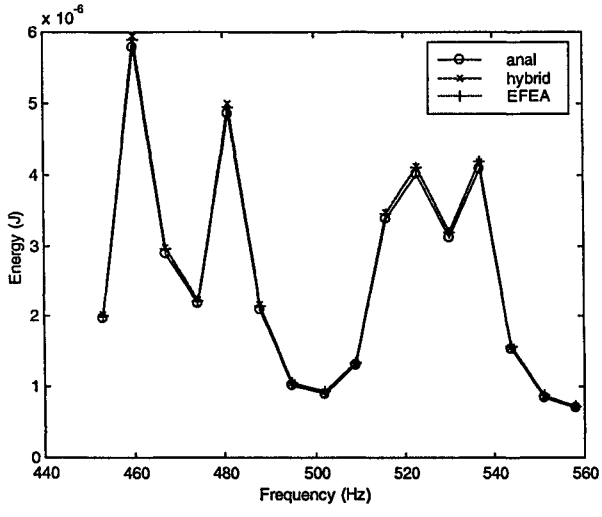

Fig. 9 Analytical, hybrid, and EFEA results for the total energy for system 4: 453–558 Hz.

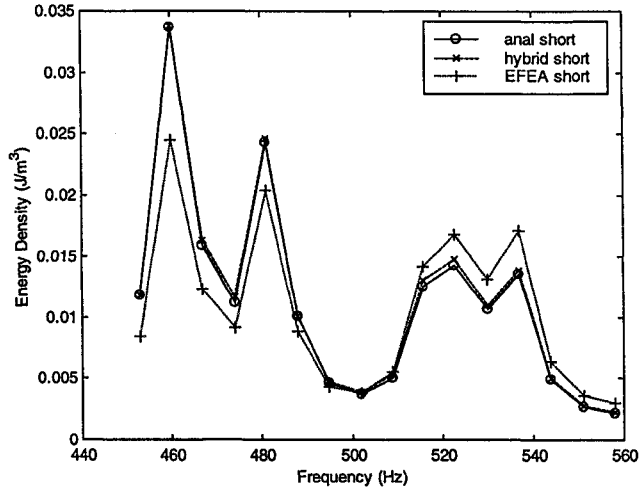

Fig. 11 Analytical, hybrid, and EFEA results for the space-averaged energy density for the short beam in system 4: 453–558 Hz.

and the EFEA solutions. Because the same amount of input power is defined as excitation in all three solutions, it is expected that the results for the total energy in the system are the same for all three methods. The differentiation in the results occurs in the predicted distribution of energy between members. The trend in the results remains the same if the length of the short member is reduced to 0.5 m (system 3). Figure 8 presents results for the average energy density in the short and long members in the frequency range 417–449 Hz. The new frequency range is selected in a manner that contains a resonant frequency of the system. Again the EFEA underpredicts the behavior of the short member, whereas the hybrid finite element analysis presents good correlation to the analytical results.

Three-Beam System

Results for a three-beam system are also presented (system 4). An analytical solution is derived for reference in a manner similar to the two-beam system. Equations (33) and (34) are employed to simulate the long members and the short member, respectively. Results for the total energy in the system are presented in Fig. 9 for a frequency range 453–558 Hz. The selected frequency range includes four resonant frequencies for the system. In two resonant frequencies, the EFEA underpredicts the behavior of the short member, and in the other two resonant frequencies, the EFEA overpredicts the behavior of the short member. Results computed by all three methods for the total energy in the system are presented first in Fig. 9. Because the same input power is specified as excitation in all three solutions, it is expected that all of them will demonstrate the same amount of total energy at each frequency. The good agreement observed in Fig. 9 validates that dissipation of energy is preserved in all three solutions. The distribution of the energy among the members differentiates the hybrid from the EFEA solution. The averaged energy density for the left long member, the short member, and the right long member are presented in Figs. 10, 11, and 12, respectively. There is excellent agreement between the hybrid and the analytical solutions for all of the members throughout the frequency range. The EFEA at two resonant frequencies underpredicts and at two resonant frequencies overpredicts the response of the short member. Results for the distribution of the space-averaged energy density over each member are presented in Figs. 13 and 14 for the resonant frequencies of 460 and 523 Hz. In the former frequency, the EFEA underpredicts the response of the short member, overpredicts the response of the excited long member, and underpredicts the response of the receiving long member. The exact opposite behavior is observed in the latter frequency. Thus, it is demonstrated that the inability of the EFEA to capture the distinct modal behavior of the short member does not only affect the response of the short member, but it also affects the power flow throughout the system. The hybrid formulation captures correctly the power transfer mechanism because it properly accounts for resonant effects, energy dissipation, power balance, and power reinjection. The good correlation between the hybrid and the analytical solution for the three-beam system also demonstrates that the power transfer coefficients computed by the hybrid joint formulation capture correctly the effect from the resonant behavior and the dissipative characteristics of the short member on the power transfer mechanism. In addition, the incoherent nature

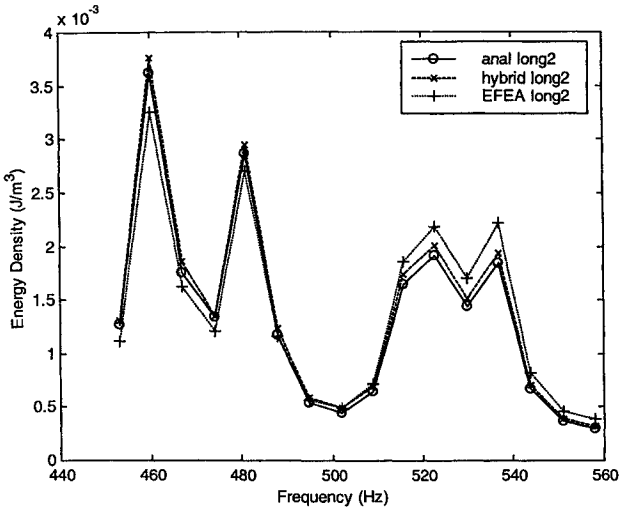

Fig. 12 Analytical, hybrid, and EFEA results for the space-averaged energy density for the right long beam in system 4: 453–558 Hz.

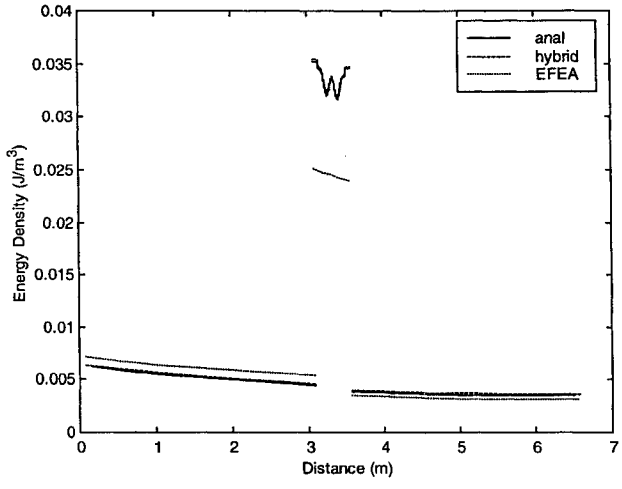

Fig. 13 Analytical, hybrid, and EFEA results for the space-averaged energy density in system 4: 460 Hz.

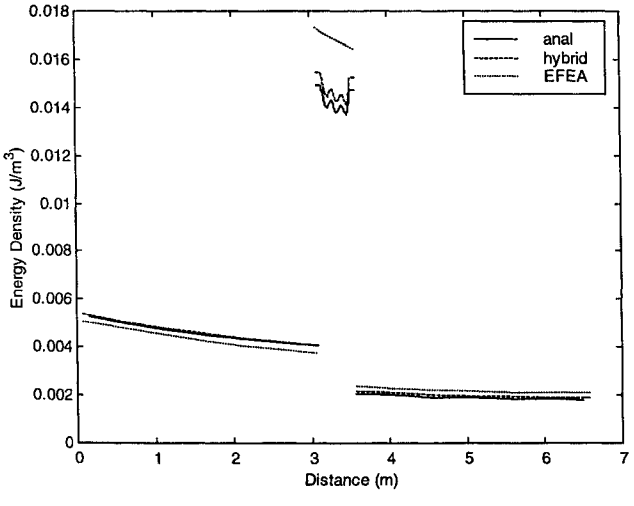

Fig. 14 Analytical, hybrid, and EFEA results for the space-averaged energy density in system 4: 523 Hz.

of the interaction between the long and the short members at the joints represents a valid assessment because in the three-beam system it is critical for capturing correctly the response of the short member and the power reinjection in the excited member.

Two more three-beam systems are analyzed by increasing the length of the short member and by extending the length of the second long member. First, the length of the short member is increased to 1 m (system 5), and the simulations are repeated. The observed trends remain the same. Results are presented for the average energy density in each member over the frequency range 446–551 Hz

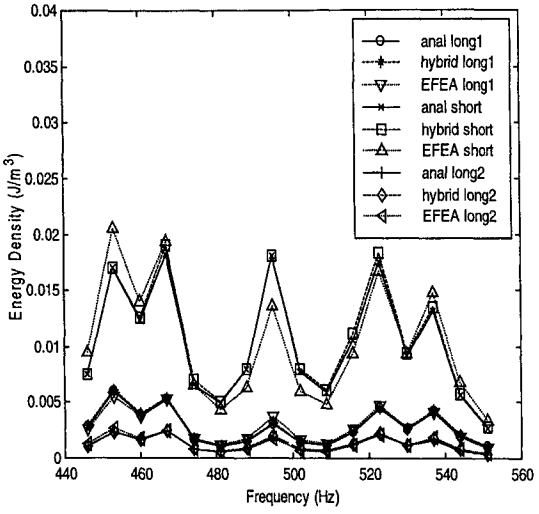

Fig. 15 Analytical, hybrid, and EFEA results for the space-averaged energy density for all members in system 5: 446–551 Hz.

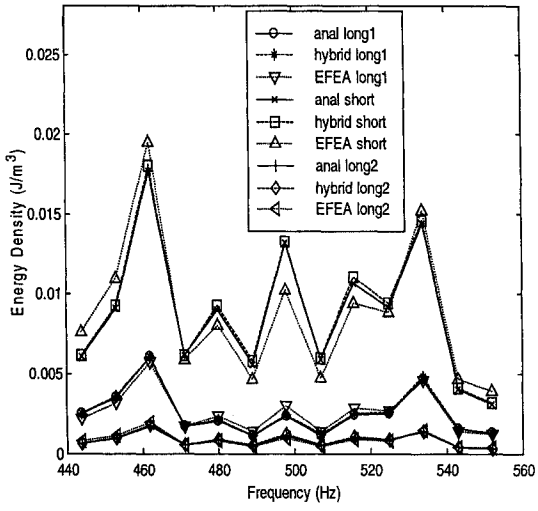

Fig. 16 Analytical, hybrid, and EFEA results for the space-averaged energy density for all members in system 6: 444–552 Hz.

(Fig. 15). The good correlation between the hybrid and the analytical solution is retained. The length of the right long member is then extended from 3 to 5.4 m (system 6). This modification alters the boundary conditions between the three members. It also increases the importance of the resonant behavior of the short member because the power transferred to the right long member strongly depends on the amount of energy in the short beam. Results for the average energy density in each member over the frequency range 444–552 Hz are presented in Fig. 16. The hybrid solution presents good correlation to the analytical results.

Overall, several configurations of colinear beam systems are analyzed. From the results it is evident that the hybrid method developed in this work captures correctly the energy in the short members, the overall response of the system, and the effect of resonant behavior in the power flow between members. The hybrid method improves significantly the numerical predictions in the midfrequency range compared to the results obtained by a high-frequency approach. The consistently good correlation between the hybrid solution and the analytical results for several system configurations and over extended frequency ranges demonstrates the proper development and implementation of the coupling between EFEA and FEA solutions and the overall validity of the hybrid formulation.

Conclusions

The theoretical development of a hybrid finite element formulation suitable for midfrequency vibration simulations is presented. During this fundamental development, the formulation for systems of colinear beams is pursued because simple analytical solutions can be readily available to validate the numerical results. During

the theoretical development, no assumptions are made that would prohibit the extension of this work to members with multiple types of waves or to members connected at arbitrary angles. Several systems of colinear beams are analyzed, and comparisons are made between analytical solutions, hybrid numerical results, and high-frequency EFEA solutions. Good correlation is observed consistently between the analytical solutions and the hybrid finite element results. The EFEA results are consistently inaccurate because the resonant effects of the short members are important to the overall behavior of the system.

Acknowledgment

This research was sponsored by Automated Analysis Corporation under Contract 970274.

References

[1]Vlahopoulos, N., Lyle, K. H., and Burley, C. L., "Technical Note: Preliminary Work for Modeling the Propellers of an Aircraft as a Noise Source in an Acoustic Boundary Element Analysis," *Noise Control Engineering Journal*, Vol. 46, No. 3, 1998, pp. 132–136.

[2]Davis, E. B., "Introducing SEA to Practising Noise Control Engineers: the Boeing Experiences," *Proceeding of Noise—Con '98*, edited by J. S. Bolton and L. Mongeau, Noise Control Foundation, Poughkeepsie, NY, 1998, pp. 531–536.

[3]Engelstad, S. P., Cunefare, K. A., Crane, S., and Powell, E. A., "Optimization Strategies for Minimum Interior Noise and Weight Using FEM/BEM," *Proceedings of Inter-Noise '95*, edited by J. S. Bolton and R. J. Bernhard, Noise Control Foundation, Poughkeepsie, NY, 1995, pp. 1205–1208.

[4]Miller, V. R., and Faulkner, L. L., "Prediction of Aircraft Interior Noise Using the Statistical Energy Analysis Method," *Proceedings of Design Engineering Technical Conference*, 1981, pp. 235–244.

[5]Vlahopoulos, N., Vallance, C., and Stark, R. D., III, "Numerical Approach for Computing Noise-Induced Vibration from Launch Environments," *Journal of Spacecraft and Rockets*, Vol. 35, No. 3, 1998, pp. 355–360.

[6]Bradford, L., and Manning, J. E., "Attenuation of the Cassini Spacecraft Acoustic Environment," *Sound and Vibration*, Vol. 10, Oct. 1996, pp. 30–37.

[7]Rodrigo, G. A., Klein, M., and Borello, G., "Vibro-Acoustic Analysis of Manned Spacecraft Using SEA," *Proceedings of NOISE–CON '94*, edited by J. Guschieri, Noise Control Foundation, Poughkeepsie, NY, 1994, pp. 887–892.

[8]Park, D. M., "VAPEPS User's Reference Manual," Ver. 5.5, Jet Propulsion Lab., Rept. JPL D-9775, California Inst. of Technology, Pasadena, CA, June 1992.

[9]Gockel, M. A. (ed.), "MSC/NASTRAN Handbook for Dynamic Analysis," Ver. 63, MacNeal–Schwendler Corp., Los Angeles, June 1983.

[10]Bathe, K. J., *Finite Element Procedures in Engineering Analysis*, Prentice–Hall, Upper Saddle River, NJ, 1982, pp. 45–65.

[11]Huebner, K. H., and Thornton, E. A., *The Finite Element Method for Engineers*, 2nd ed., Wiley, New York, 1982, pp. 233–242.

[12]Burroughs, C. B., Fischer, R. W., and Kern, F. R., "An Introduction to Statistical Energy Analysis," *Journal of the Acoustical Society of America*, Vol. 101, No. 4, 1997, pp. 1779–1789.

[13]Radcliffe, C. J., and Huang, X. L., "Putting Statistics into the Statistical Energy Analysis of Automotive Vehicles," *Journal of Vibration and Acoustics*, Vol. 119, Oct. 1997, pp. 629–634.

[14]Thomas, R. S., Pan, J., Moeller, M. J., and Nolan, T. W., "Implementing and Improving Statistical Energy Analysis Models using Quality Technology," *Noise Control Engineering Journal*, Vol. 45, No. 1, 1997, pp. 25–34.

[15]Woodhouse, J., "An Approach to the Theoretical Background of Statistical Energy Analysis Applied to Structural Vibration," *Journal of the Acoustical Society of America*, Vol. 69, No. 6, 1991, pp. 1695–1709.

[16]Lyon, R., *Statistical Energy Analysis of Dynamical Systems: Theory and Application*, MIT Press, Cambridge, MA, 1975, pp. 72–104.

[17]Bouthier, O. M., and Bernhard, R. J., "Simple Models of the Energetics of Transversely Vibrating Plates," *Journal of Sound and Vibration*, Vol. 182, No. 1, 1995, pp. 149–164.

[18]Huff, J. E., and Bernhard, R. J., "Prediction of High Frequency Vibrations in Coupled Plates using Energy Finite Element," *Proceedings of Inter–Noise '95*, edited by J. S. Bolton and R. J. Bernhard, Noise Control Foundation, Poughkeepsie, NY, 1995, pp. 1221–1226.

[19]Bouthier, O. M., "Energetics of Vibrating Systems," Ph.D. Dissertation, Mechanical Engineering Dept., Purdue Univ., Lafayette, IN, Aug. 1992.

[20]Bouthier, O. M., and Bernhard, R. J., "Models of Space Averaged Energetics of Plates," *AIAA Journal*, Vol. 30, No. 3, 1992, pp. 138–146.

[21]Nefske, D. J., and Sung, S. H., "Power Flow Finite Element Analysis of Dynamic Systems: Basic Theory and Applications to Beams," *Journal of Vibration, Acoustics, Stress and Reliability*, Vol. 111, 1989, pp. 94–106.

[22]Vlahopoulos, N., Zhao, X., and Allen, T., "An Approach for Evaluating Power Transfer Coefficients for Spot-Welded Joints in an Energy Finite Element Formulation," *Journal of Sound and Vibration*, Vol. 220, No. 1, 1999, pp. 135–154.

[23]Vlahopoulos, N., Garza-Rios, L. O., and Mollo, C., "Numerical Implementation, Validation, and Marine Applications of an Energy Finite Element Formulation," *Journal of Ship Research* (to be published).

[24]Mace, B. R., "The Statistical Energy Analysis of Two Continuous One-Dimensional Subsystems," *Journal of Sound and Vibration*, Vol. 166, No. 3, 1993, pp. 429–461.

[25]Cremer, L., Heckl, M., and Ungar, E. E., *Structure Borne Sound*, Springer–Verlag, Berlin, 1973, pp. 132–134.

[26]Fredo, C. R., "A SEA-like Approach for the Derivation of Energy Flow Coefficients with a Finite Element Model," *Journal of Sound and Vibration*, Vol. 199, No. 4, 1997, pp. 645–666.

[27]DeLange, K., Sas, P., and Vandepitte, D., "The Use of Wave-Absorbing Elements for the Evaluation of Transmission Characteristics of Beam Junctions," *Journal of Vibration and Acoustics*, Vol. 119, 1997, pp. 293–303.

[28]Steel, J. A., and Craik, R. J. M., "Statistical Energy Analysis of Structure-Borne Sound Transmission by Finite Element Methods," *Journal of Sound and Vibration*, Vol. 178, No. 4, 1994, pp. 553–561.

[29]Simmons, C., "Structure-Borne Sound Transmission through Plate Junctions and Estimates of SEA Coupling Loss Factors Using the Finite Element Method," *Journal of Sound and Vibration*, Vol. 144, No. 2, 1991, pp. 215–227.

[30]Manning, J. E., "Calculation of Statistical Energy Analysis Parameters Using Finite Element and Boundary Element Models," *1990 Proceedings of International Congress in Air- and Structure-Borne Sound and Vibration*, edited by M. J. Crocker and P. K. Raju, International Sound and Vibration Congress, Mechanical Engineering Dept., Auburn Univ., Auburn, AL, 1990, pp. 771–778.

[31]Seeman, W., "Transmission and Reflection Coefficients for Longitudinal Waves Obtained by a Combination of Refined Rod Theory and FEM," *Journal of Sound and Vibration*, Vol. 197, No. 5, 1996, pp. 571–587.

[32]Thouverez, F., Viktorovitch, M., and Jezequal, L., "A Random Boundary Element Formulation for Assembled Rods and Beams in the Mid Frequency Range," *New Advances in Modal Synthesis of Large Structures*, edited by L. Jezequal, Balkema, Rotterdam, The Netherlands, 1997, pp. 435–444.

[33]Lu, L., "Dynamic Substructuring by FEA/SEA," *Vehicle Noise*, edited by S. H. Sung, K. H. Hsu, and R. F. Keltie, American Society of Mechanical Engineers, New York, 1990, pp. 9–12.

[34]Sun, J. S., Wang, C., and Sun, Z. H., "Power Flow between Three Series Coupled Oscillators," *Journal of Sound and Vibration*, Vol. 189, No. 2, 1996, pp. 215–229.

[35]Cho, P., "Energy Flow Analysis of Coupled Structures," Ph.D. Dissertation, Mechanical Engineering Dept., Purdue Univ., Lafayette, IN, Dec. 1993.

[36]Mace, B. R., "Power Flow Between Two Coupled Beams," *Journal of Sound and Vibration*, Vol. 159, No. 2, 1992, pp. 305–325.

S. Saigal
Associate Editor